European Association for the Development of Renewable Energies, Environment and Power Quality

International Conference on Renewable Energies and Power Quality (ICREPQ'09)

Valencia (Spain), 15th to 17th April, 2009

A Control Strategy for Combined Series-Parallel Active Filter System under Non-Periodic Conditions

M. Ucar, S. Ozdemir and E. Ozdemir

Electrical Education Department
Technical Education Faculty, Kocaeli University
41380, Umuttepe, Turkey
Phone/Fax number:+90262 3032275 / :+90262 3032203
e-mail: mucar@kocaeli.edu.tr, sozaslan@kocaeli.edu.tr, eozdemir@kocaeli.edu.tr

Abstract. In this study, generalized non-active power theory based control strategy is proposed for a 3-phase 4-wire Combined Series-Parallel Active Filter (CSPAF) system using a Three-Dimensional (3D) Space Vector Pulse Width Modulation (SVPWM). The CSPAF system consists of a Series Active Filter (SAF) and a Parallel Active Filter (PAF) combination connected a common Direct Current (DC) link for simultaneous compensating the source voltage and the load current. The generalized non-active power theory was applied in previous studies for the PAF control, in this study the theory is used for the CSPAF system control under non-sinusoidal and non-periodic current and voltage conditions. The closed loop control algorithm for the proposed CSPAF system has been described to direct control of filtering performance by measuring source currents and load voltages for the PAF and the SAF, respectively. The proposed control strategy has been verified by simulating the CSPAF system in Matlab/Simulink environment.

Key words

Harmonics, unbalance, reactive power compensation, non-periodic, active filter, 3D-SVPWM.

1. Introduction

The large use of non-linear loads and power electronic converters has increased the generation of non-sinusoidal and non-periodic currents and voltages in electric power systems. Generally, power electronic converters generate harmonic components which frequencies that are integer multiplies of the line frequency. However, in some cases, such as line commutated three-phase thyristor based rectifiers, arc furnaces and welding machines, the line currents may contain both frequency lower and higher than the line frequency but not the integer multiple of line frequency. These currents interact with the impedance of the power distribution system and disturb voltage waveforms at Point of Common Coupling (PCC) that can affect other loads. These waveforms are considered as non-periodic, although mathematically the currents may still have a periodic waveform, but in any event, the period of the currents is not equal to the period of the line voltage [1], [2]. In this paper, the generalised instantaneous non-active power theory is used for the CSPAF system under non-sinusoidal and non-periodic load current and source voltage conditions.

The CSPAF system consists of back-to-back connection of SAF and PAF with a common DC link. While the PAF compensates current quality problems of load and regulating of DC link, the SAF compensates voltage quality problems of utility [3], [4]. The system configuration of the CSPAF system is shown in Fig. 1.

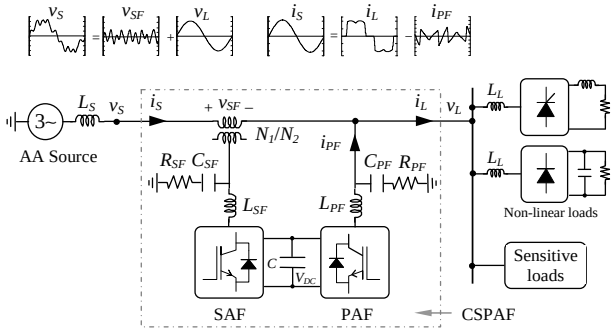

Fig. 1. System configuration of the CSPAF system.

In 3-phase 3-wire systems, conventional SVPWM method, which is based on $\alpha\beta$ plane, has been widely used to reduce ripples and to get fixed switching frequency. In this study, the 3D-SVPWM scheme is used for controlling the CSPAF system, which uses two 3-leg 4-wire Voltage Source Inverter (VSI) because the zero sequence components must be controlled [5]. In the closed loop control scheme of the proposed CSPAF system, source currents and load voltages are measured and filtering performance is controlled directly. The CSPAF system provides minimum harmonics of these currents and voltages.

2. Generalized Non-Active Power Theory

The generalised non-active power theory [6] is based on Fryze's theory of non-active power/current [7] and is an extension of the theory proposed in [8] [9]. Voltage vector $v(t)$ and current vector $i(t)$ in a 3-phase system,

$$v(t) = [v_1(t), v_2(t), v_3(t)]^T, \tag{1}$$

$$i(t) = [i_1(t), i_2(t), i_3(t)]^T. \tag{2}$$

The instantaneous power $p(t)$ and the average power $P(t)$ is defined as the average value of the instantaneous power $p(t)$ over the averaging interval $[t\text{-}T_c, t]$, that is

$$p(t) = v^T(t)\, i(t) = \sum_{p=1}^{3} v_p(t)\, i_p(t), \tag{3}$$

$$P(t) = \frac{1}{T_c} \int_{t-T_c}^{t} p(\tau)\, d\tau. \tag{4}$$

The averaging time interval T_c can be chosen arbitrarily from zero to infinity for compensation of periodic or non-periodic waveforms, and for different T_c's, the resulting active current and non-active current will have different characteristics [6]. The instantaneous active current $i_a(t)$ and non-active current $i_n(t)$ are given (5) and (6).

$$i_a(t) = \frac{P(t)}{V_p^2(t)} v_p(t) \tag{5}$$

$$i_n(t) = i(t) - i_a(t) \tag{6}$$

In (5), voltage $v_p(t)$ is the reference voltage, which is chosen on the basis of the characteristics of the system and the desired compensation results. $V_p(t)$ is the corresponding rms value of the reference voltage $v_p(t)$, that is

$$V_p(t) = \sqrt{\frac{1}{T_c} \int_{t-T_c}^{t} v_p{}^T(\tau)\, v_p(\tau)\, d\tau}. \tag{7}$$

The instantaneous non-active power $p_n(t)$ and the average non-active power $P_n(t)$ is defined over the averaging interval $[t\text{-}T_c, t]$, that is

$$p_n(t) = v^T(t)\, i_n(t) = \sum_{p=1}^{3} v_p(t)\, i_{np}(t), \tag{8}$$

$$P_n(t) = \frac{1}{T_c} \int_{t-T_c}^{t} p_n(\tau)\, d\tau. \tag{9}$$

The definitions in the instantaneous non-active power theory are all consistent with the standard definitions for three-phase fundamental sinusoidal systems and are valid in various cases, such as single-phase systems, non-sinusoidal systems, and non-periodic systems as well, by changing the averaging interval T_c and the reference voltage $v_p(t)$ [10]. In this theory, all the definitions are instantaneous values; therefore, they are suitable for real-time control.

3. 3D-SVPWM Algorithm

In this paper, the 3D-SVPWM algorithm is utilized for controlling the CSPAF system, which uses two 3-leg 4-wire VSI. The switching vectors of the 3-leg 4-wire VSI are shown into a 3D plane in Fig. 2. The eight switching vectors are distributed in the $\alpha\beta0$ space and the zero switching vectors V_0 and V_7 are in opposite directions. Since there is a zero axis in the 3D space, two zero switching vectors can be used independently to control the zero sequence voltage [5].

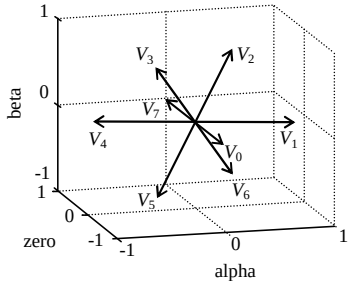

Fig. 2. Switching vectors in 3D space.

The instantaneous voltage can be transformed to the $\alpha\beta0$ 3D space by using (10).

$$\begin{bmatrix} v_0 \\ v_\alpha \\ v_\beta \end{bmatrix} = \sqrt{\frac{2}{3}} \begin{bmatrix} 1/\sqrt{2} & 1/\sqrt{2} & 1/\sqrt{2} \\ 1 & -1/2 & -1/2 \\ 0 & \sqrt{3}/2 & -\sqrt{3}/2 \end{bmatrix} \begin{bmatrix} v_a \\ v_b \\ v_c \end{bmatrix} \tag{10}$$

The reference vector in the $\alpha\beta0$ 3D space can be written as,

$$\overline{V}_R(k) = i.v_\alpha + j.v_\beta + k.v_0. \tag{11}$$

Once the reference vector V_R has been determined, it can be reflected the $\alpha\beta$ plane as shown in Fig. 3 to decide which sector and which active switching vectors are to be selected [5].

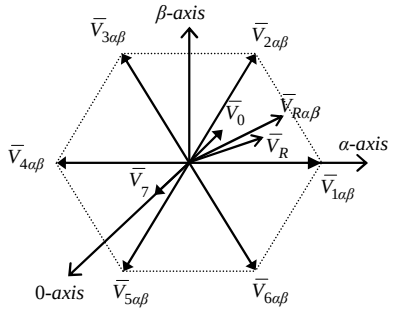

Fig. 3. 3D-SVPWM method in the 3-leg 4-wire VSI.

Two zero-switching vectors V_0 and V_7 with different effective times t_0 and t_7 can synthesize the reflection of the reference vector in the zero axis. Along with the different switching functions, the reference space vector $V_R(k)$ is presented in Table I.

TABLE I. Switching functions and switching voltage space vectors

S_a	S_b	S_c	V_R	Switching vectors
1	0	0	$(i.2 + j.0 + k.(-\frac{\sqrt{2}}{2})).\frac{V_{dc}}{\sqrt{6}}$	V_1
1	1	0	$(i.1 + j.\sqrt{3} + k.(\frac{\sqrt{2}}{2})).\frac{V_{dc}}{\sqrt{6}}$	V_2
0	1	0	$(i.(-1) + j.\sqrt{3} + k.(-\frac{\sqrt{2}}{2})).\frac{V_{dc}}{\sqrt{6}}$	V_3
0	1	1	$(i.(-2) + j.0 + k.(\frac{\sqrt{2}}{2})).\frac{V_{dc}}{\sqrt{6}}$	V_4
0	0	1	$(i.(-1) + j.(-\sqrt{3}) + k.(-\frac{\sqrt{2}}{2})).\frac{V_{dc}}{\sqrt{6}}$	V_5
1	0	1	$(i.1 + j.(-\sqrt{3}) + k.(\frac{\sqrt{2}}{2})).\frac{V_{dc}}{\sqrt{6}}$	V_6
1	1	1	$(i.0 + j.0 + k.1).\frac{\sqrt{3}}{2}V_{dc}$	V_7
0	0	0	$(i.0 + j.0 + k.(-1)).\frac{\sqrt{3}}{2}V_{dc}$	V_0

In Fig. 3, the reference voltage vector V_R is located in a sector in which the four switching states (V_0, V_7, V_1 and V_2) are adjacent to the reference vector. The effective switching time of each switching vector, within PWM switching period, T_s, can be obtained from an equation (12), (13) [5].

$$\overline{V}_0.t_0 + \overline{V}_1.t_1 + \overline{V}_2.t_2 + \overline{V}_7.t_7 = \overline{V}_R.t_s \tag{12}$$

$$t_0 + t_1 + t_2 + t_7 = t_s \tag{13}$$

(14)-(17) show the equations involved in the calculation of switching time of each involved switching vector for reference vector happens in sector I.

$$t_1 = \frac{\sqrt{2}}{V_{dc}} \cdot t_s \cdot \left[(\frac{\sqrt{3}}{2}) \cdot v_{R\alpha} + (-\frac{1}{2}) \cdot v_{R\beta} \right] \tag{14}$$

$$t_1 = \frac{\sqrt{2}}{V_{dc}} \cdot t_s \cdot v_{R\beta} \tag{15}$$

$$t_7 - t_0 = \frac{2}{\sqrt{3}} \cdot \frac{v_{R0}}{V_{dc}} \cdot t_s - (t_2 - t_1)/3 \tag{16}$$

$$t_7 + t_0 = t_s - (t_2 + t_1) \tag{17}$$

The selected switching vectors can be applied in a sequence optimized to reduce switching loss or achieve a better voltage Total Harmonic Distortion (THD). Symmetrical sequencing gives the lowest THD output, due to the fact that all switching vectors are arranged symmetrically [11]. So this sequencing method is chosen in this paper. In symmetrical sequencing strategy, the switching sequence is arranged as V_0 - V_1 - V_2 - V_7 - V_7 - V_2 - V_1 - V_0. Fig. 4 shows the sequencing of switching states for a time period of T_s for sector I.

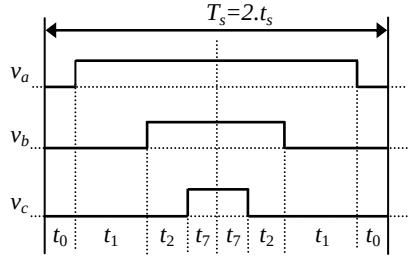

Fig. 4. PWM switching time sequence.

4. Control of the CSPAF System

In this study, the CSPAF system, which has two 3-leg 4-wire VSI, uses generalised non-active power theory based current and voltage control with the 3D-SVPWM scheme.

A. Voltage control strategy

Voltage control block diagram is shown in Fig. 5. The non-sinusoidal, unbalanced and/or non-periodic load voltages (v_{La}, v_{Lb}, v_{Lc}) is applied to Phase Locked Loop (PLL) circuit and fundamental positive sequence currents (i_{a1+}, i_{b1+}, i_{c1+}), used as a reference current $i_p(t)$ and the same phase with the fundamental positive sequence load voltage (v_{La1+}, v_{Lb1+}, v_{Lc1+}) and unity amplitude are obtained. Effective value of reference current $I_p(t)$ is

$$I_p(t) = \sqrt{\frac{1}{T_c} \int_{t-T_c}^{t} i_p{}^T(\tau) i_p(\tau) d\tau} \tag{18}$$

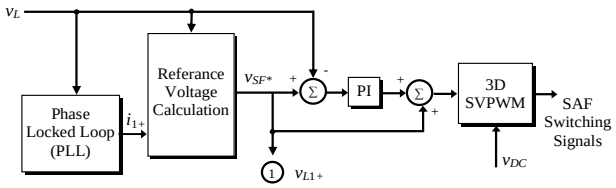

Fig. 5. Voltage control block diagram.

The average power calculated given (4) by using this reference currents and source voltages. Desired sinusoidal load voltages (v_{La1+}, v_{Lb1+}, v_{Lc1+}) as compensation reference voltages (v_{SFa*}, v_{SFb*}, v_{SFc*}) of SAF, is derived by using (19) from amplitude and phase angle of fundamental positive sequence component of the load voltages. Reference voltage is compared load

voltages and applied to 3D-SVPWM and thus SAF switching signals are obtained.

$$v_a(t) = \frac{P(t)}{I_p^2(t)} i_p(t) \tag{19}$$

B. Current control strategy

The average power calculated given (4) by using source currents and fundamental positive sequence (v_{La1+}, v_{Lb1+}, v_{Lc1+}) load voltages over the averaging interval [t-T_c, t]. Desired sinusoidal source currents (i_{Sa1+}, i_{Sb1+}, i_{Sc1+}) are derived by using (5). Also, the additional active current $i_{ca}(t)$ required to meet the losses in (20) is drawn from the source by regulating the DC link voltage v_{DC} to the reference V_{DC}. A Proportional Integral (PI) controller is used to regulate the DC link voltage v_{DC}. Thus, the compensation reference currents (i_{PFa*}, i_{PFb*}, i_{PFc*}) of PAF is obtained.

The reference currents are compared source currents to realize the closed loop control scheme. Then, using 3D-SVPWM controller, PAF switching signals are obtained. Current control block diagram of the CSPAF system is shown in Fig. 6. The CSPAF system Matlab/Simulink block diagram is shown in Fig. 7.

$$i_{ca}(t) = v_L[K_P(V_{DC} - v_{DC}) + K_I \int_0^t (V_{DC} - v_{DC})dt] \tag{20}$$

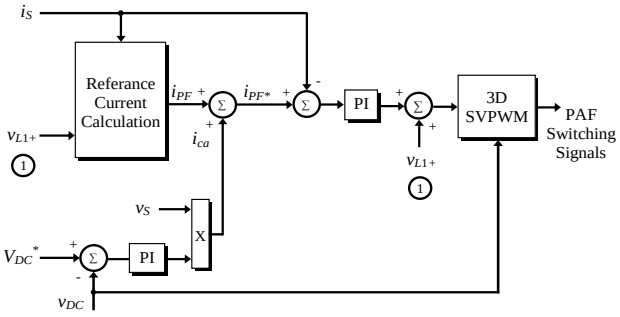

Fig. 6. Current control block diagram.

5. Periodic Current and Voltage

For compensation of periodic currents and voltages with fundamental period T, using a compensation period T_c that is a multiple of $T/2$ is enough for complete compensation [6]. In this study, 3-phase source voltage components is given in Table II. 3-phase RL loaded tyristor rectifier and 1-phase RC loaded diode rectifier in each phase connected 3-phase 4-wire power system. Thyristor rectifier firing angles are 30°.

TABLE II. 3-phase source voltage components

Fundamental	Unbalance (%)	Harmonics (%)						
50 Hz	20	5.	7.	9.	11.	13.	17.	19.
220 V		10	7,5	15	5	2,5	1,25	1

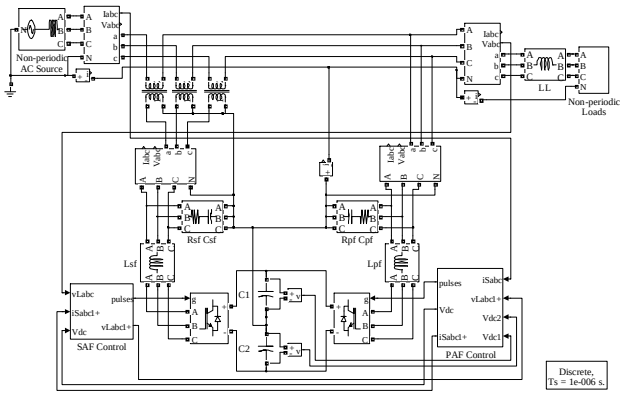

Fig. 7. The CSPAF system Matlab/Simulink block diagram.

Fig. 8 demonstrate the simulation results for the periodic current and voltage compensation. 3-phase source current and load voltage is sinusoidal and balanced and neutral current eliminated after compensation. Table III shows a summary of measured components.

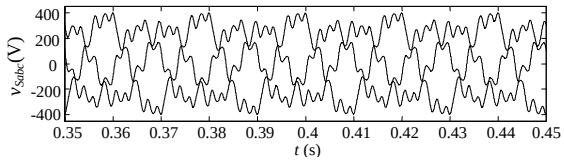

(a) 3-phase source voltage waveforms.

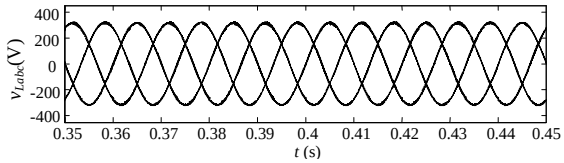

(b) 3-phase load voltages after compensation.

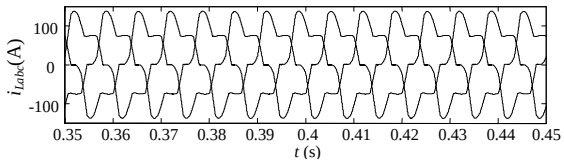

(c) 3-phase load current waveforms.

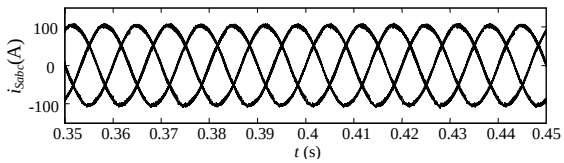

(d) 3-phase source currents after compensation.

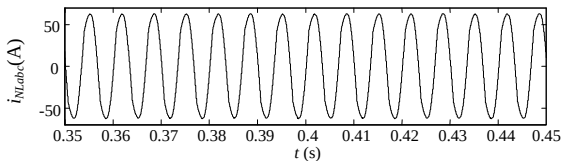

(e) Load neutral current waveforms.

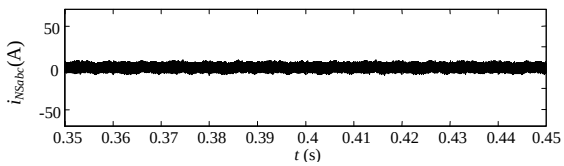

(f) Source neutral current after compensation.

Fig. 8. Periodic voltage and current compensation.

TABLE III. Summary of measured values under periodic current and voltage condition

		Load Currents (I_L)	Source Currents (I_S)
THD (%)	*a*	28,97	4,34
	b	29,08	4,48
	c	29,04	4,34
	n	165,30	-
RMS (A)	*a*	81,05	73,74
	b	81,01	73,78
	c	81,59	74,03
	n	47,21	-
		Source Voltages (V_S)	Load Voltages (V_L)
THD (%)	*a*	22,20	2,21
	b	22,20	2,30
	c	16,96	2,13
RMS (V)	*a*	206,5	219,1
	b	206,5	219,2
	c	267,7	219,5

6. Non-Periodic Current and Voltage

A. Sub-harmonic current and voltages

The sub-harmonic currents are (frequency lower than fundamental frequency) typically generated by power electronic converters. The main feature of these non-periodic currents is that the currents may have a repetitive period. When the fundamental frequency of the source voltage is an odd multiple of the sub-harmonic frequency, the minimum T_c for complete compensation is 1/2 of the common period of both f_s and f_{sub}. When f_s is an even multiple of f_{sub}, the minimum T_c for complete compensation is the common period of both f_s and f_{sub} [6].

In this study, 3-phase source voltage and load current components are given in Table IV. Sub-harmonic current and voltage compensation simulation results are shown in Fig. 9. The sub-harmonic component can be completely compensated by choosing T_c=2.5T, and the source currents and load voltages are balanced and sinusoidal. Additionally, the neutral current component is compensated.

TABLE IV. 3-phase source voltage and load current values

Parameters	Fundamental	Sub-harmonic
Freq. (Hz)	50	10
Currents	50 A	% 20
Voltages	220 V	% 20

B. Stochastic non-periodic currents and voltages

The arc furnace load currents may contain stochastic non-periodic currents (frequency higher than fundamental frequency but not an integer multiple of it). Theoretically, the period T of a non-periodic load is infinite [12]. The non-active components in these loads cannot be completely compensated by choosing T_c as $T/2$ or T, or even several multiples of T. Choosing that period as may result in an acceptable both source current and load voltage which are quite close to a sine wave. If T_c is large enough, increasing T_c further will not typically improve the compensation results significantly [10].

In this work, 3-phase source voltage and load current components is given in Table V. Fig. 10 shows the stochastic non-periodic voltage and current compensation choosing the period as T_c=5T. After compensation, load voltages and source currents are balanced and almost sinusoidal with low THD. In addition, source neutral current have been reduced considerably. The system parameters used for the simulation are given in Table VI.

TABLE V. 3-phase source voltage and load current components

Parameters	Fund.	Components (%)				
Freq. (Hz)	50	104	117	134	147	250
Currents	50 A	30	40	20	20	50
Voltages	220 V	7,5	10	5	5	12,5

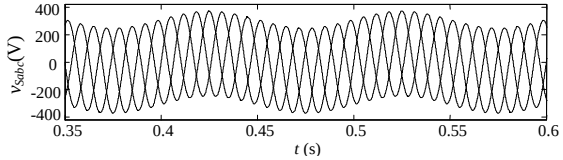

(a) 3-phase source voltage waveforms.

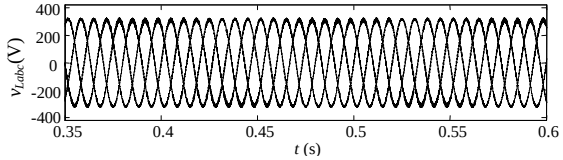

(b) 3-phase load voltages after compensation.

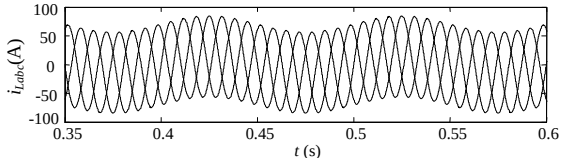

(c) 3-phase load current waveforms.

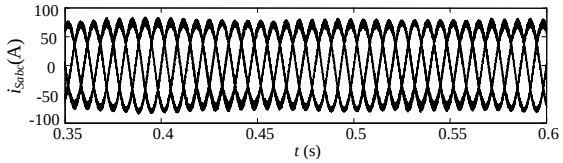

(e) Load neutral current waveforms.

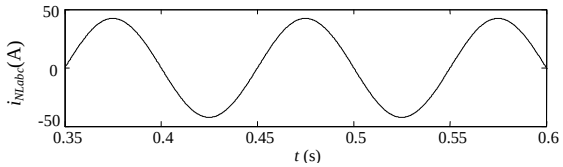

(e) Load neutral current waveforms.

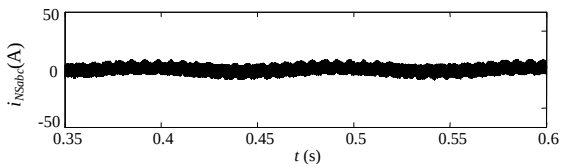

(f) Source neutral current after compensation.

Fig. 9. Sub-harmonic voltage and current compensation.

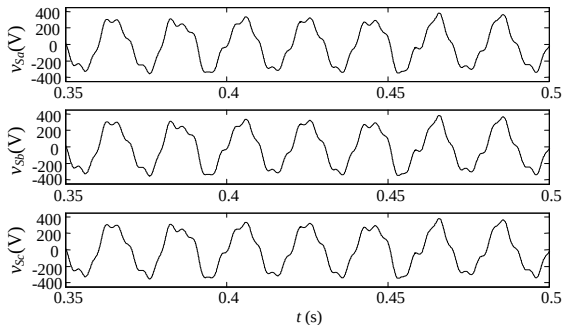

(a) 3-phase source voltage waveforms.

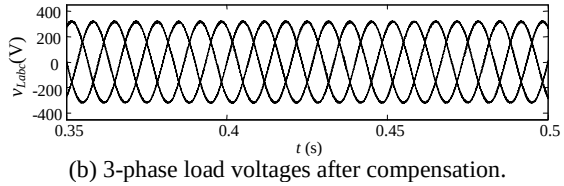

(b) 3-phase load voltages after compensation.

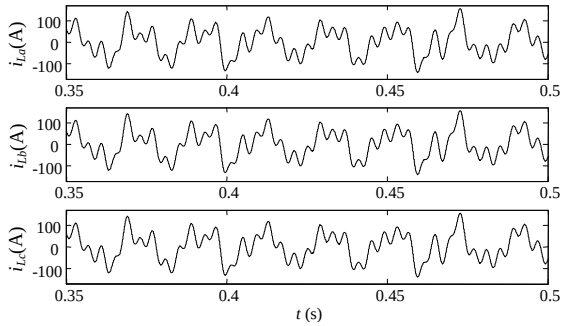

(c) 3-phase load current waveforms.

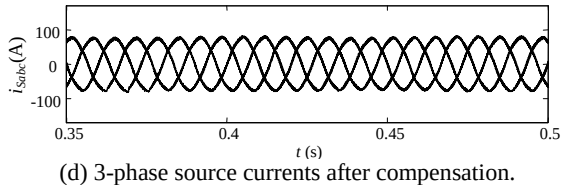

(d) 3-phase source currents after compensation.

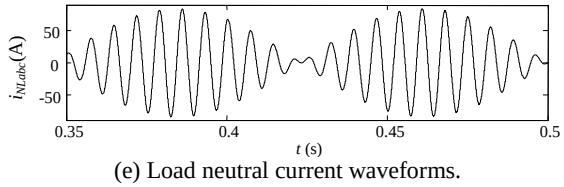

(e) Load neutral current waveforms.

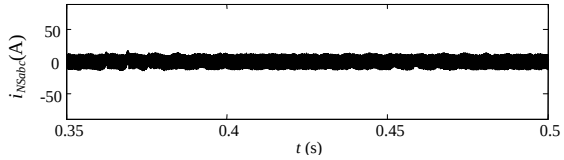

(f) Source neutral current after compensation.

Fig. 10. Stochastics non-periodic voltage and current compensation.

TABLE VI. The system parameters

Power system	V_{Sabc}, f_s, L_s	220V, 50Hz, 50μH
Series transformer	N_1/N_2	1
SAF AA filter	L_{SF}, R_{SF}, C_{SF}	2mH, 2Ω, 30μF
PAF AA filter	L_{PF}, R_{PF}, C_{PF}	1mH, 1Ω, 30μF
DC bus	V_{DC},C_1, C_2	800V, 5600μF
Switching freq.	f_{SAF}, f_{PAF}	10kHz
3-phase thristor	L_{L1}, $L_{DC,}$ R_{DC1}	3mH, 20mH, 5Ω
1-phase diode	L_{L2}, $C_{DC,}$ R_{DC2}	3mH, 470μF, 15Ω

7. Conclusion

In this paper, the generalized non-active power theory, which is applicable to sinusoidal or non-sinusoidal, periodic or non-periodic, balanced or unbalanced electrical systems, is presented. It has been applied to the 3-phase 4-wire CSPAF system with the 3D-SVPWM to get fixed switching frequency. The theory is adapted to different compensation objectives by changing the averaging interval T_c. The closed loop control algorithm has been described by measuring source currents and load voltages in the proposed CSPAF system to direct control of filtering performance. The simulation results based on Matlab/Simulink software are presented to show the effectiveness of the CSPAF system for the compensation of a variety of non-sinusoidal and non-periodic voltages and currents in power systems.

Acknowledgement

This work is supported by TUBITAK Research Fund, (Project No: 108E083).

References

[1] Watanabe, E. H. and Aredes, M., "Compensation of Nonperiodic Currents Using The Instantaneous Power Theory", IEEE Power Engineering Soc. Summer Meeting, 2000, 994-999.

[2] Czarnecki, L. S., "Non-Periodic Currents: Their Properties, Identification and Compensation Fundamentals", IEEE Power Engineering Soc. Summer Meeting, 2000, 971-976.

[3] Fujita, H. and Akagi, H., "The Unified Power Quality Conditioner: The Integration of Series and Shunt Active Filters", IEEE Trans. on Power Electr**.**, 13 (2), 1998.

[4] Aredes, M., "Active Power Line Conditioners", Ph.D. Dissertation, Technischen Universität**,** Berlin, 1996.

[5] C. Zhan, A. Arulampalam, V. K. Ramachandaramurthy, C. Fitzer, M. Barnes, N. Jenkins, "Novel voltage space vector PWM algorithm of 3-phase 4-wire power conditioner", IEEE Power Eng. Soc., pp. 1045-1050, 2001.

[6] Xu, Y., Tolbert, L. M., Peng, F. Z., Chiasson, J. N. and Chen, J. "Compensation-Based Non-Active Power Definition", IEEE Power Electr. Letter, 1 (2), 45-50, 2003.

[7] Fryze, S. "Active, Reactive, and Apparent Power in Non-Sinusoidal Systems", Przeglad Elektrot., 7, 193-203 (in Polish), 1931.

[8] Peng, F. Z., and Tolbert, L. M. "Compensation of Non-Active Current In Power Systems - Definitions from Compensation Standpoint", IEEE Power Eng. Soc. Summer Meeting, 2000, 983-987.

[9] Xu, Y., Tolbert, L. M., Chiasson, J. N., Campbell, J. B. and Peng, F. Z., "A Generalised Instantaneous Non-Active Power Theory for STATCOM", Electric Power Applications, IET, 853-861, 2007.

[10] Xu, Y., Tolbert, L. M., Chiasson, J. N., Campbell, J. B. and Peng, F.Z., "Active Filter Implementation Using a Generalized Nonactive Power Theory", IEEE Industry Applications Conference, 2006, 153-160.

[11] H.Pinheiro, F. Botteron, C. Rech. Schuch and et al., "Space Vector Modulation for Voltage-Source Inverter: A Unified Approach," IECON02, Industrial Electronics Society, IEEE 2002, 28th Annual Conference.

[12] Tolbert, L. M., Xu, Y., Chen, J., Peng, F. Z, Chiasson, J. N., "Compensation of Irregular Currents with Active Filters," IEEE Power Engineering Society General Meeting, 2003, 1278-1283.